Research Square

Preprints are preliminary reports that have not undergone peer review.
They should not be considered conclusive, used to inform clinical practice,
or referenced by the media as validated information.

Synthesis and Application in Cell Imaging of a Fluorescent Probe for Detection of Zn2+/S2- and Viscosity

Siyi WEN
Xihua University
Yan TANG
Xihua University
Dingxin QIU
Xihua University
Gong Chen
Civil Aviation Flight University of China
Ke Su
Aba Teachers College
Huizhen WANG
578527840@qq.com
Xihua University

Research Article

Keywords: Schiff base, fluorescent probe, Zn2+/S2−, viscosity, cell imaging

Posted Date: August 28th, 2026

DOI: https://doi.org/10.21203/rs.3.rs-10622722/v1

License: This work is licensed under a Creative Commons Attribution 4.0 International License.
Read Full License

Additional Declarations: No competing interests reported.

Synthesis and Application in Cell Imaging of a Fluorescent Probe for Detection of Zn^{2+}/S^{2-} and Viscosity

Siyi WEN[a], Yan TANG[a], Dingxin QIU[a], Gong Chen[b], Ke Su[c*], Huizhen WANG[a*]

a. School of Science, Asymmetric Synthesis and Chiral technology Key Laboratory of Sichuan Province, Xihua University, Chengdu 610039; P. R. China. E-mail: 578527840@qq.com;

b. College of Flight Technology, Civil Aviation Flight University of China;

c. School of Resource and Environment, Aba Teachers College, Aba 623002, P. R. China. E-mail: 1107244969@qq.com.

Abstract: A fluorescent probe **DBH** with Schiff base structure was synthesized using 3,4-dimethoxybenzohydrazide and 3,5-di-tert-butyl-2-hydroxybenzaldehyde as starting materials. Spectroscopic studies showed that probe **DBH** can specifically recognize Zn^{2+} and S^{2-} (DMF/H_2O = 5:5), exhibiting significant fluorescence enhancement effects for both. The detection limits (LOD) were determined to be 4.19×10^{-7} mol/L for Zn^{2+} and 1.45×10^{-7} mol/L for S^{2-}. The binding mechanism of **DBH** with Zn^{2+}/S^{2-} was investigated through Job's plot, NMR titration, mass spectrometry, and DFT calculations. Furthermore, probe's low cytotoxicity and good biocompatibility enable the detection of exogenous Zn^{2+}/S^{2-} in living cells. In addition, the probe exhibits a distinct viscosity-responsive behavior, showing linear relationship between fluorescence intensity and system viscosity. Probe **DBH** has potential for real-time monitoring of styrene polymerization progress.

Keywords: Schiff base; fluorescent probe; Zn^{2+}/S^{2-}; viscosity; cell imaging

1 Introduction

Among the metal ions involved in physiological functions, zinc ions (Zn^{2+}) play a critical role in numerous biological processes [1]. Zinc is essential for physiological processes such as gene transcription, neural signal transduction, and immune function. Studies have shown that Zn^{2+} is crucial for children's intellectual development, physical growth, and also closely associated with diabetes and neurodegenerative diseases. Zn^{2+} play important roles synaptic plasticity, and their concentration imbalance may lead to neurological disorders such as Alzheimer's disease and Parkinson's disease [2-4]. In environmental field, excess Zn^{2+} can pollute soil and water systems, affecting plant growth and the survival of aquatic organisms. Although traditional Zn^{2+} detection

techniques offer high analytical precision, they suffer from high costs, complex procedures, and long analysis times. In contrast, fluorescence probe technology, with its advantages of high sensitivity and visual detection, provides a new and effective means for Zn^{2+} detection, enabling rapid and accurate determination of zinc ions in biological samples [5–7].

Sulfide ions (S^{2-}) are an important component of sulfur cycle in ecosystems. In environment, S^{2-} primarily originate from the oxidation of sulfur-containing minerals, industrial wastewater, and the metabolic activities of anaerobic microorganisms [8–9]. Excessive S^{2-} in water bodies can lead to water quality deterioration, generate hydrogen sulfide gas, and also exert toxicity on aquatic organisms, disrupting the aquatic ecological balance [8, 10]. In living organisms, S^{2-} participate in various physiological processes, such as redox reactions and the regulation of enzyme activity [11, 12]. However, abnormal levels of sulfide ions are associated with many diseases. For example, in nervous system, excessive S^{2-} may be involved in the pathological processes of neurodegenerative diseases [13–16]. Traditional detection methods for S^{2-} face challenges such as poor selectivity and low sensitivity, making it difficult to meet the detection requirements in complex systems. Fluorescence probe technology has become a research hotspot for detecting sulfide ions, offering the potential to deeply explore the mechanisms of action of sulfide ions in physiological and pathological processes and to achieve effective detection of sulfide ions in environmental and biological samples.

Polymer viscosity, as a key parameter determining processing performance and product quality, makes its online monitoring crucial for the control of polymerization processes. Traditional offline detection methods such as rotational and capillary techniques generally suffer from response lag and limitations in adapting to high-viscosity or micro-scale systems [17]. Among these, rotational rheometers are constrained by a narrow shear rate range and high-pressure sealing issues, capillary rheometers require complex calibration, while viscometry face drawbacks such as long operation times, susceptibility to degradation, and wall adsorption interference [18,19]. The aforementioned methods cannot provide real-time feedback on the reaction process. In contrast, fluorescence probe technology, with its advantages of high sensitivity, visualization, and in situ microscopic imaging, offers a direct means for real-time

monitoring of micro-viscosity changes, demonstrating unique application potential in the dynamic tracking of polymerization processes [17,20].

Fluorescent probes have proven to be valuable tools for viscosity detection [21], making them an essential component in various critical industries such as food processing [22–25], biopharmaceuticals, and materials manufacturing. Their main advantages lie in high sensitivity and in situ microscopic viscosity monitoring, providing a basis for quality control, process optimization, and fundamental scientific research [22, 24, 26, 27].

Schiff bases are a class of organic compounds characterized by the imine group (RC=N) as their structural feature, synthesized via the condensation dehydration reaction of aldehydes/ketones containing active carbonyl groups with primary amines [28–30]. The lone pair electrons on the nitrogen atom in Schiff base molecules endow them with strong coordination ability, allowing them to form stable complexes with various metal ions [5, 6, 21]. On this basis, a novel Schiff base compound was synthesized and utilized to investigate the interaction mechanism. Notably, this probe exhibits a rapid and selective response to Zn^{2+}/S^{2-}, accompanied by a significant fluorescence "turn-on" effect. Furthermore, probe **DBH** has potential for real-time monitoring of styrene polymerization progress.

2 Experimental

2.1 Chemicals and Instruments

3,4-Dimethoxybenzohydrazide, A.R., Aladdin; 3,5-Di-tert-butyl-2-hydroxy benzal dehyde, A.R., Beijing InnoChem Science & Technology Co., Ltd.; Zinc sulfate heptahydrate, A.R., Chengdu Kelong Chemical Reagent Factory; Sodium sulfide, A.R., Chengdu Kelong Chemical Reagent Factory

Nuclear magnetic resonance spectrometer (Bruker, Bruker Corporation, Switzerland); Electrospray ionization mass spectrometer (1290 Infinity II/ 6470, Agilent Technologies Inc., USA); Fluorescence spectrophotometer (F-4600, Shimadzu Corporation, Japan); UV-Vis spectrophotometer (UV-2700, Shimadzu Corporation, Japan); Fourier transform infrared spectrometer (Nicolet IS20, Thermo Fisher Scientific Inc., USA).

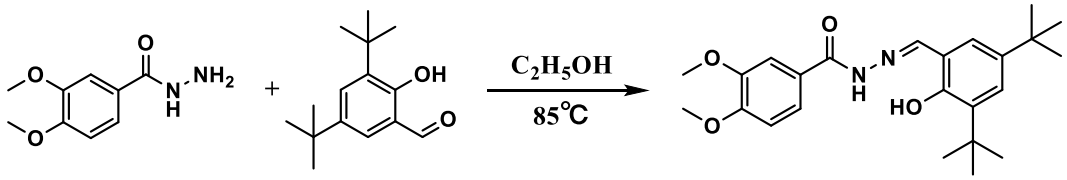
2.2 Synthesis of Probe Compound **DBH**

3,4-dimethoxybenzohydrazide (0.2025 g; 1.0 mmol) was transferred to a 50 mL round-bottom flask, and anhydrous ethanol (5.0 mL) was added to fully dissolve the

hydrazide, followed by stirring. The reaction system was heated to 85 °C and maintained at this temperature with stirring for 10 mins. Then, 3, 5-di-tert-butyl-2-hydroxy-benzal-dehyde (0.2811 g; 1.2 mmol) was added, and the reaction was continued for another 20 mins. Three drops of glacial acetic acid were added, and the reaction system was heated under reflux at 85 °C for 4h. The reaction progress was monitored by thin-layer chromatography (TLC). After the reaction was complete, the mixture was cooled to room temperature. The crude product was collected by suction filtration, washed three times with anhydrous ethanol, and dried to obtain a pale yellow solid powder. MP: 212.8-214.1 °C; the reaction yield was 85.3% (Scheme 1).

^{1}H NMR (400 MHz, DMSO-d6): δ ppm 12.32 (s, 1H), 12.05 (s, 1H), 8.59 (s, 1H), 7.61 (dd, J = 8.4, 2.0 Hz, 1H), 7.52 (d, J = 2.1 Hz, 1H), 7.32 (d, J = 2.4 Hz, 1H), 7.22 (d, J = 2.3 Hz, 1H), 7.13 (d, J = 8.5 Hz, 1H), 3.86 (d, J = 2.3 Hz, 6H), 1.42 (s, 9H), 1.29 (s, 9H).

^{13}C NMR (400MHz，DMSO-d6): δ ppm 162.75 (s) , 155.70 (s) , 153.35 (s) , 153.20 (s) , 153.10 (s) , 149.10 (s) , 148.63 (s) , 129.40 (s) , 128.93(s) , 126.00 (s) , 125.57 (s) , 116.75 (s) , 116.32 (s) , 105.89 (s) , 105.43 (s) , 60.74 (s) , 60.50(s) , 56.68 (s) , 56.39 (s) , 34.38 (s) , 34.09 (s) , 31.84 (s) , 31.59 (s) , 31.55 (s). IR (KBr), 3440cm^{-1}, 3190 cm^{-1}, 2960 cm^{-1}, 1640 cm^{-1}, 1270 cm^{-1}, 1020 cm^{-1}, 772cm^{-1}. HR-MS: calculated for $C_{24}H_{32}N_2O_4$ $[M + H]^+$ = 413.2440, found 413.3957.



Scheme 1. Synthetic route of compound **DBH**

2.3 Preparation of Solutions

Probe **DBH** was dissolved in DMF to prepare stock solution with concentration of 1.0 × 10^{-3} mol/L, stored in dark.

Preparation of ion solutions: 22 metal cations（K^+、Ca^{2+}、Na^+、Mg^{2+}、Al^{3+}、Zn^{2+}、Fe^{3+}、Hg^{2+}、Mn^{2+}、Ni^{2+}、Cu^{2+}、Co^{2+}、Cd^{2+}、Ag^+、Ba^{2+}、Cr^{3+}、Pb^{2+}、Li^+、Mo^{6+}、Sr^{2+}、Sn^{2+}、Ce^{3+}）and 21 anions（S^{2-}、F^-、Cl^-、Br^-、I^-、CO^{3-}、SO_4^{2-}、SO_3^{2-}、PO_4^{3-}、HPO_4^{2-}、$H_2PO_4^-$、NO_3^-、NO_2^-、CH_3COO^-、HCO_3^-、SCN^-、OH^-、CN^-、ClO^-、H_2O_2/O_2^{2-}、KO_2/O_2^-）were prepared as solutions with a concentration of 1.0 × 10^{-1} mol·L^{-1} and stored in dark.

2.4 Spectroscopic Test Methods

UV-Vis absorption spectrum test parameter settings: scanning range of 300-800 nm. Fluorescence spectrum test parameter settings: excitation wavelength set to 380 nm, scanning range of 300-800 nm, scan rate of 1200 nm/min, and both excitation and emission monochromator slit widths set to 5.0 nm.

3 Results and Discussion

3.1 The Recognition of Metal Ions

To investigate the selective recognition ability of **DBH** toward different metal ions, fluorescence and UV-Vis absorption were analyzed in a H_2O/DMF = 5:5 system, with the probe **DBH** concentration at 1.0×10^{-5} mol/L and metal ion concentrations at 1.0×10^{-4} mol/L (Fig. 1.). The λ_{max} was 314 nm, the λ_{em} was 502 nm, and the Stokes shift was 188 nm. The results showed that the fluorescence of probe **DBH** was significantly enhanced upon interaction with Zn^{2+}, while it remained essentially unchanged upon interaction with other metal ions. This indicates that probe **DBH** can selectively recognize Zn^{2+}.

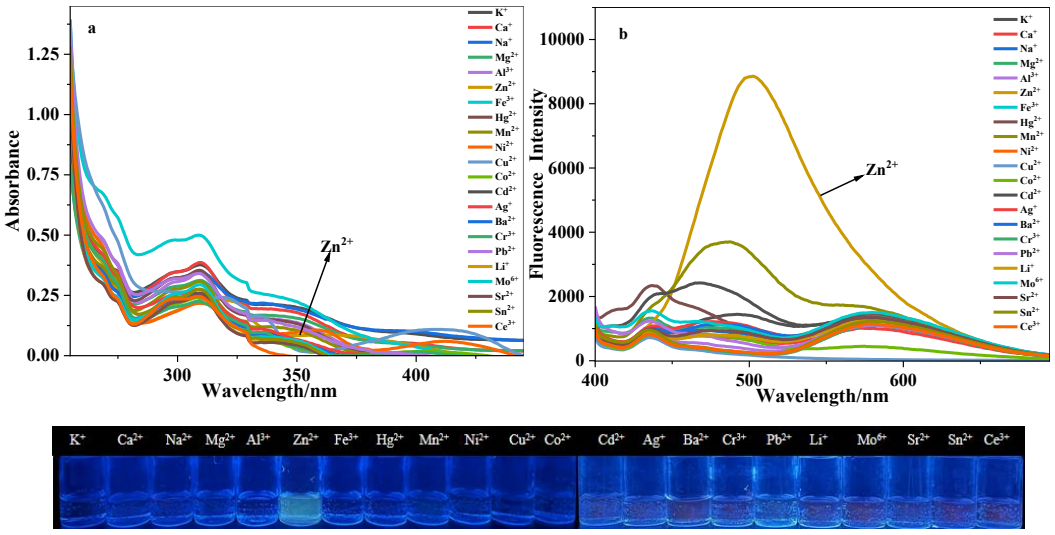


Fig. 1. UV-Vis (a) and fluorescence (b) spectra of probe **DBH** upon interaction with different ions

（λ_{ex}=380nm, H_2O/DMF=5:5）

3.2 Sensitivity of Probe **DBH** for Zn^{2+} Detection

To investigate the sensitivity of probe **DBH** for Zn^{2+} detection, fluorescence spectra were measured in the presence of varying concentrations of Zn^{2+} (Fig. 2.). Results showed that as the concentration of Zn^{2+} increased, the fluorescence emission gradually intensified, exhibiting a significant linear correlation. Within the Zn^{2+}

concentration range of 0.6-2.6 × 10^{-5} mol/L, a linear relationship was plotted with the Zn^{2+} concentration as abscissa and the fluorescence intensity at 462 nm as ordinate. The obtained linear correlation coefficient R^2 was 0.98164. The detection limit (LOD) was calculated according to the formula LOD = 3σ/K (K = 203.25 × 10^5; standard deviation of the blank sample σ = 2.8452), giving a value of 4.19 × 10^{-7} mol/L.

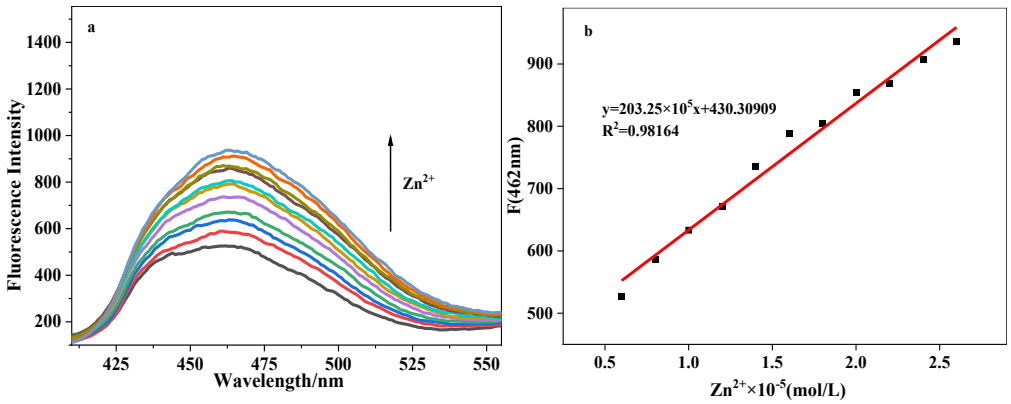


Fig. 2. Fluorescence spectra of probe **DBH** with increasing Zn^{2+} concentration (a) and linear relationship plot (b)（λ_{ex}=380nm, H_2O/DMF=5:5）

3.3 The Recognition of Anions

To verify the recognition ability of probe **DBH** toward anions, fluorescence and UV-Vis tests were conducted in a H_2O/DMF = 5:5 system with probe **DBH** concentration at 1.0 × 10^{-5} mol/L and anion concentrations at 1.0 × 10^{-5} mol/L (Fig. 3.). Results showed that the fluorescence of probe **DBH** was significantly enhanced upon interaction with S^{2-}, while it remained essentially unchanged upon interaction with other anions. This indicates that probe **DBH** can selectively recognize S^{2-}.

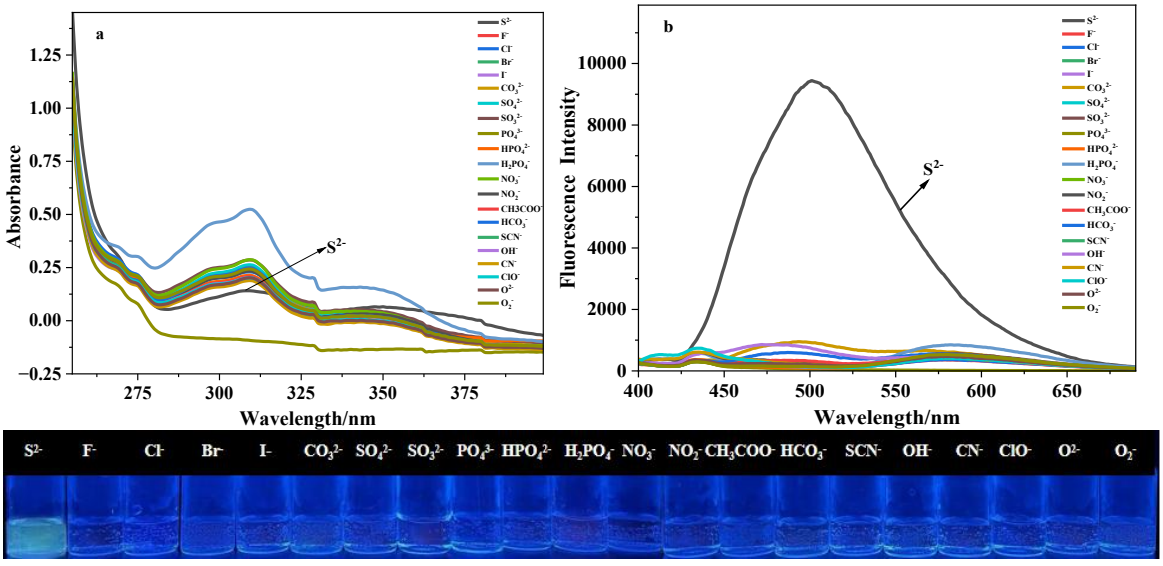


Figure 3 UV-Vis (a) and fluorescence (b) spectra of probe **DBH** interacting with different anions（λ_{ex}=380nm，H_2O/DMF=5:5）

3.4 Sensitivity of Probe **DBH** for S^{2-} Detection

To investigate the sensitivity of probe **DBH** for S^{2-} detection, fluorescence spectra were measured in the presence of varying concentrations of S^{2-} (Fig. 4.). Results showed that as the concentration of S^{2-} increased, the fluorescence emission gradually intensified. Within the S^{2-} concentration range of 8.5×10^{-5} to 1.15×10^{-4}mol/L, a linear relationship was plotted with the S^{2-} concentration as abscissa and the fluorescence intensity at 500 nm as ordinate. The linear correlation coefficient R^2 was 0.99191. Based on the detection limit formula LOD = 3σ/K (K = 5.88371×10^7; standard deviation of the blank sample σ = 2.8452), the detection limit (LOD) was calculated to be 1.45×10^{-7}mol/L.

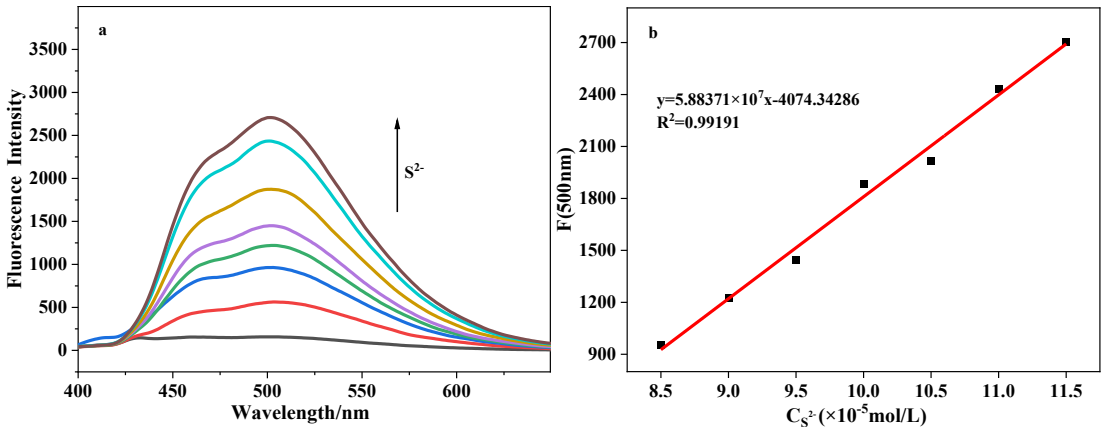


Fig. 4. Fluorescence spectra of probe **DBH** with increasing S^{2-} concentration (a) and linear relationship plot (b)（λ_{ex}=380nm，H_2O/DMSO=8:2）

3.5 Investigation of the Mechanism

First, the Job's plot test for **DBH** and Zn^{2+} was conducted. As shown in Fig. S8, when the molar fraction of Zn^{2+} to [Zn^{2+} + **DBH**] reached 0.5, the fluorescence intensity reached its maximum, confirming that **DBH** binds to Zn^{2+} in a 1:1 ratio. The mass spectrometry result in positive ion mode is shown in Fig. S5, where the peak at 475.3184 corresponds to [**DBH** + Zn-H]$^+$, further supporting the conclusion that the coordination ratio is indeed 1:1.

Furthermore, ^{1}H NMR titration analysis was performed. Zn^{2+} (0.5 equiv., 1.0 equiv., and 1.5 equiv.) was added to a DMSO-d_6 solution containing 0.01 mmol/L of probe **DBH**, and NMR spectra were recorded (Fig. 5a.). The results showed that the signal peak intensity of -OH at δ=8.59 ppm significantly decreased, indicating coordination between -OH and Zn^{2+}. Comprehensive studies confirmed that the **DBH** molecule achieves specific capture of Zn^{2+} through a bidentate coordination mode involving O atom of -OH and N atom of =N-. Specifically, the -OH acts as an electron donor via its O atom to form a coordination bond with Zn^{2+}, while the N atom occupies the remaining coordination site of Zn^{2+} through its lone pair electrons, ultimately forming a six-membered ring chelate structure (Fig. 6.).

To elucidate the coordination mechanism between probe **DBH** and S^{2-}, ^1H NMR titration was employed. S^{2-} (0.5 equiv., 1.0 equiv., and 1.5 equiv.) was added to a DMSO-d_6 solution containing 0.01 mmol/L of probe **DBH**, and NMR spectra were recorded (Fig. 5b.). Results showed that the signal peak of –OH at δ=12.0 ppm completely disappeared, indicating that the S^{2-} abstracted the proton from -OH, generating HS^- and a phenolate anion (Fig. 6.). This deprotonation disrupted the original intramolecular hydrogen bond network of probe **DBH**. The electrons on O atom delocalized into the benzene ring, inducing conjugation of the benzene ring and increasing the electron cloud density. This mechanism not only led to the disappearance of proton signal in the downfield region of probe **DBH** but also produced a significant colorimetric response, providing a molecular design basis for the development of highly selective fluorescent probes for sulfide ions.

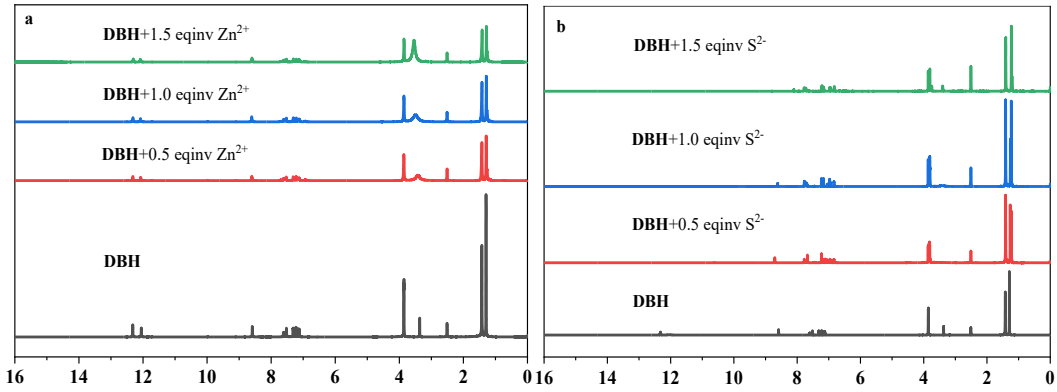


Fig. 5. ^1H NMR spectra of probe **DBH** with different equivalents of Zn^{2+} (a) and S^{2-} (b).

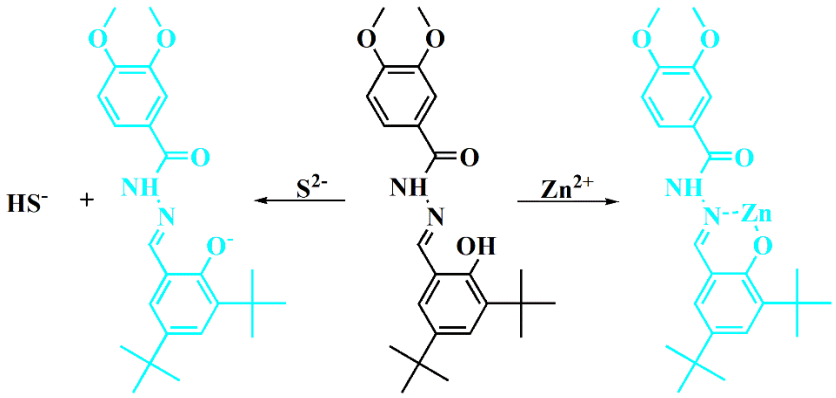


Fig. 6. Proposed mechanism for the binding of probe **DBH** with Zn^{2+} and S^{2-}

3.8 DFT Calculations

To investigate the reaction mechanism, density functional theory (DFT) calculations were performed using MS software for molecular geometry optimization. Molecular orbital analysis was carried out using the GGA-PBE functional and the DNP basis set. For the **DBH** system, the energies of the highest occupied molecular orbital (HOMO) and the lowest unoccupied molecular orbital (LUMO) were -4.816 eV and -1.252 eV, respectively, with an energy gap of 3.564 eV. However, for the **DBH**+Zn^{2+} complex, the HOMO and LUMO energies were -4.816 eV and -2.667 eV, respectively, resulting in a reduced energy gap of 2.149 eV. For the **DBH**+S^{2-} complex, the HOMO and LUMO energies were -4.354 eV and -2.231 eV, respectively, leading to a reduced energy gap of 2.123 eV (see Fig. 7.). These results indicate that both **DBH**+Zn^{2+} and **DBH**+S^{2-} are more stable than **DBH** alone. This conclusion is supported by the Job's plot and ^{1}H NMR results.

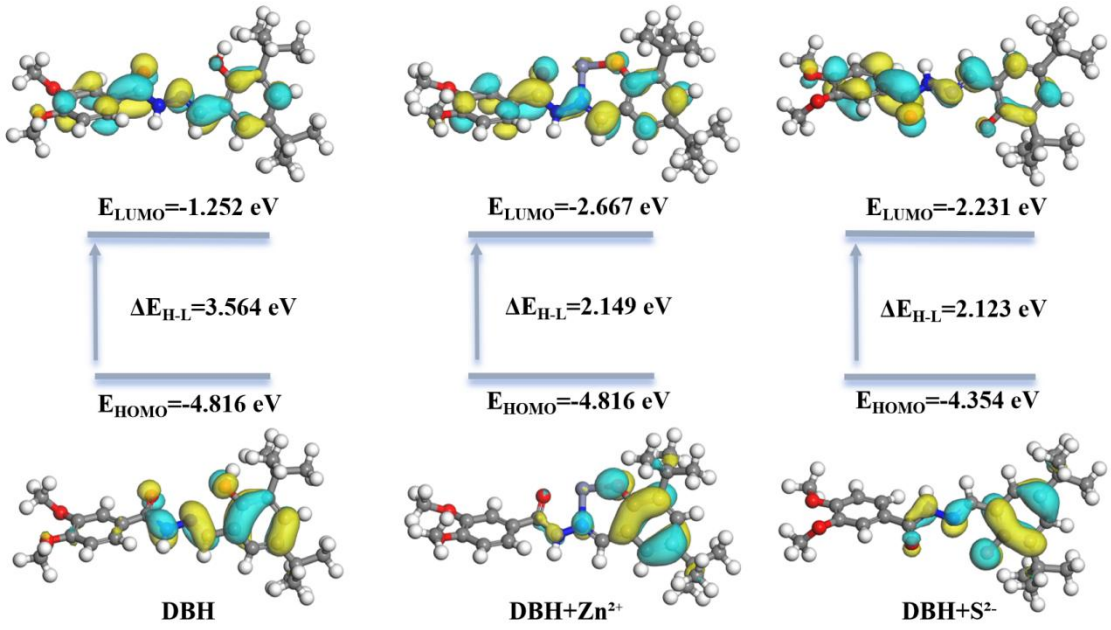


Fig. 7. Electron density maps of HOMO and LUMO structures and band gap energies of **DBH**/**DBH**+Zn^{2+}/**DBH**+S^{2-}

3.9 Viscosity Response of Probe **DBH**

To investigate the relationship between fluorescence of probe **DBH** and system viscosity, the fluorescence intensity was measured in methanol-glycerol mixed systems

with different ratios. As the glycerol content in the mixed system gradually increased, the fluorescence of probe **DBH** gradually intensified (Fig. 8a.). In the methanol-glycerol ratio range of 20% to 65%, a linear relationship was plotted with GLY/(MeOH+GLY) as abscissa and the fluorescence intensity at 432 nm as ordinate. The linear correlation coefficient R^2 =0.99062. This phenomenon can be attributed to the fact that as viscosity increases, the collision frequency between excited-state **DBH** molecules decreases, reducing non-radiative decay processes and thereby affecting the fluorescence intensity.

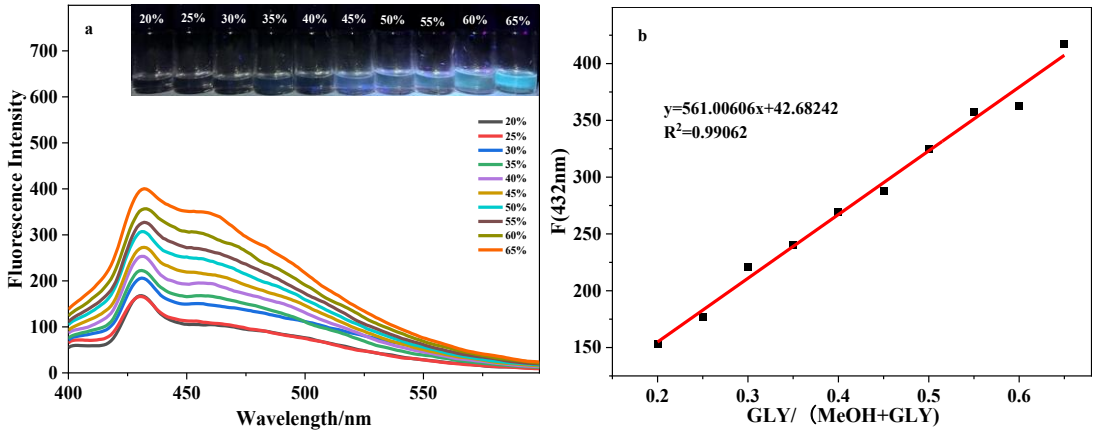


Fig. 8. Fluorescence spectra of probe **DBH** with increasing GLY/(MeOH+GLY) ratio (a) and linear relationship plot (b) (λ_{ex} = 380 nm)

3.10 Application for Polymerization Process Monitoring

To investigate the application of probe **DBH** in monitoring the polymerization process, following experiment was conducted: styrene monomer was mixed with probe **DBH**, followed by the addition of initiator BPO (the concentration of probe **DBH** was 5.0 × 10^{-2} mol/L). The mixture was first pre-gelated at 90 °C, and then transferred to a 50 °C environment to complete the final gelation. The experimental results showed a significant change in fluorescence intensity before and after polymerization (Fig. 9.). Before polymerization, both the probe molecules and monomers were in a disordered, free-moving state. After polymerization, the monomers formed long-chain molecules and became “fixed” in the polymer network, with restricted rotation. This fluorescence enhancement originates from the restricted of **DBH** molecular rotation. Future research will focus on designing fluorescent probes sensitive to viscosity changes to achieve visual monitoring of the polymerization process.

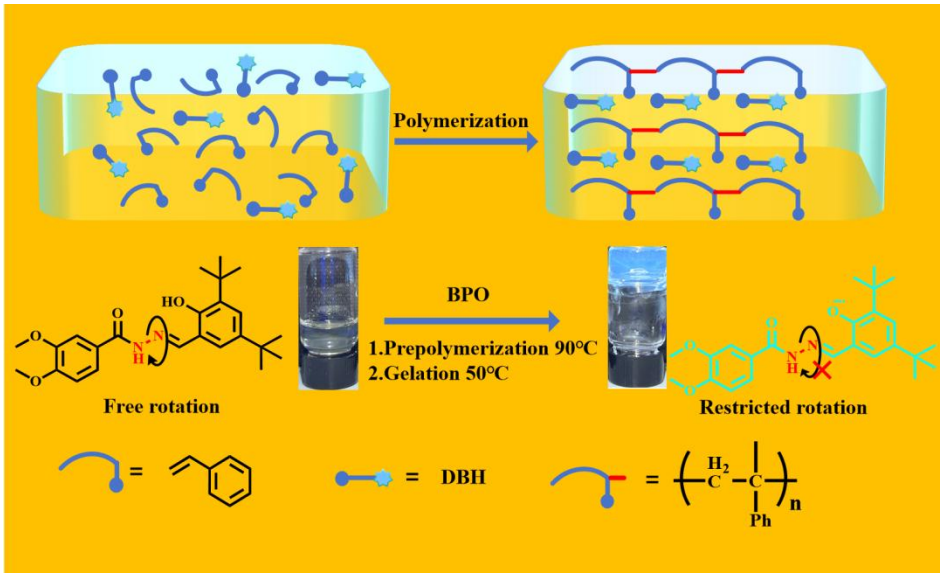


Fig. 9. Schematic diagram of viscosity detection using probe **DBH**

3.11 Cell Imaging

MTT assay was performed to evaluate the cytotoxicity of probe **DBH**. As shown in Fig. S10, even at a high concentration (100 μM), probe **DBH** exhibited no significant cytotoxic effects on normal human liver cells (L929) and human hepatocellular carcinoma cells (HepG2). To explore the ability of probe **DBH** to detect exogenous Zn^{2+} and S^{2-}, HepG2 cells were selected for fluorescence microscopy imaging. As shown in Fig. 10, after incubation of **DBH** with HepG2 cells, no fluorescence was observed in the green channel. However, when HepG2 cells were cultured with 50 μM and 100 μM of Zn^{2+} or S^{2-}, clear fluorescence signals were detected in the green channel. These results indicate that probe **DBH** possesses good biocompatibility and the ability for exogenous qualitative detection of Zn^{2+} and S^{2-}.

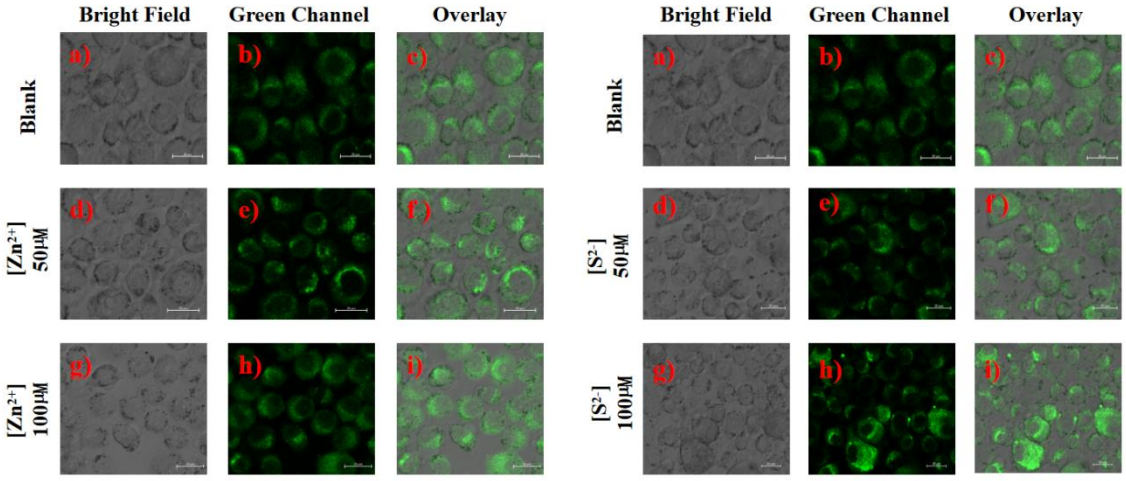


Fig. 10. Confocal fluorescence imaging: Left (a-c) **DBH** staining (20 μM, 30 min); (d-f) **DBH**

staining (20 μM, 30 min) and Zn^{2+} treatment (50 μM, 30 min); (g-i) **DBH** staining (20 μM, 30 min) and Zn^{2+} treatment (100 μM, 30 min). λex = 405 nm, scale bar: 30 μm. Right (a-c) **DBH** staining (20 μM, 30 min); (d-f) **DBH** staining (20 μM, 30 min) and S^{2-} treatment (50 μM, 30 min); (g-i) **DBH** staining (20 μM, 30 min) and S^{2-} treatment (100 μM, 30 min). λex = 405 nm, scale bar: 30 μm.

4 Conclusion

In summary, a Schiff base fluorescent probe **DBH** capable of detecting Zn^{2+}/S^{2-} and viscosity was developed. Spectroscopic studies showed that probe **DBH** can selectively recognize Zn^{2+} and S^{2-}, producing significant fluorescence enhancement. The detection limits were as low as 4.19×10^{-7} mol/L for Zn^{2+} and 1.45×10^{-7} mol/L for S^{2-}. The interaction mechanisms of **DBH** with Zn^{2+}/S^{2-} were determined through ^{1}H NMR titration, Job's plot, HRMS, and DFT calculations. Additionally, a strong linear relationship was observed between the fluorescence intensity of probe **DBH** and viscosity. Styrene polymerization experiments demonstrated that **DBH** has the potential for visual monitoring of the polymerization process. Furthermore, probe **DBH** exhibits low cytotoxicity and good biocompatibility, making it suitable for detecting exogenous Zn^{2+} and S^{2-} in living cells. Probe **DBH** shows great potential for bioimaging of Zn^{2+} and S^{2-} in biological systems.

Supporting Information

Supporting information includes experimental section, **DBH** and **DBH** + Zn^{2+} characterization spectra (for example: FTIR, ^{1}H NMR, ^{13}C NMR and HRMS spectra), the influence of anion and pH on spectral performance, and job's curve of probe **DBH** + Zn^{2+}.

Acknowledgements

This work was financially supported by the Special Project for Guiding Local Science and Technology Development by the Central Government of Sichuan Province(2024ZYD0302), the Ministry of Education Chunhui Project (No. 191630) and the Sichuan Provincial Department of Education Project (No. 18ZB0571).

Declaration of competing interest

The authors declare that they have no known competing financial interests or personal relationships that could have appeared to influence the work reported in this paper.

References

[1] Li L, Zhang Q, Sun G, et al. Double-clamp Schiff base ligand engineered Ru (II) complex exhibiting Zn^{2+}-activated fluorescence for selective Zn^{2+} detection and live-cell imaging[J]. Talanta, 2026;305:129669.

[2] Chausmer A B. Zinc, Insulin and Diabetes[J]. Journal of the American College of Nutrition, 1998;17(2):109–15.

[3] Khan M Z. A possible significant role of zinc and GPR39 zinc sensing receptor in Alzheimer disease and epilepsy[J]. Biomedicine & Pharmacotherapy, 2016;79:263–72.

[4] Bloem B R, Okun M S, Klein C. Parkinson's disease[J]. The Lancet, 2021;397(10291):2284–303.

[5] Wang H, Yang T, Ni S, et al. A “Turn-On” fluorescent probe for detection and removal of Zn^{2+} in aqueous and its application in living cells[J]. Spectrochimica Acta Part A: Molecular and Biomolecular Spectroscopy, 2022;280:121501.

[6] Wang H, Guo Y, Tang Y, et al. The design of multifunctional fluorescent probe for detecting Zn^{2+}/ ClO^{-}/H_2O and application in high-security level information encryption[J]. Dyes and Pigments, 2024;223:111909.

[7] Wen J R, Hua Q Y, Ding S, et al. Recent Advances in Fluorescent Probes for Zinc Ions Based on Various Response Mechanisms[J]. Critical reviews in analytical chemistry, 2023.

[8] Zak D, Hupfer M, Cabezas A, et al. Sulphate in freshwater ecosystems: A review of sources, biogeochemical cycles, ecotoxicological effects and bioremediation[J]. Earth-science reviews, 2021;212.

[9] Twible L E, Whaley-Martin K, Chen L X, et al. pH and thiosulfate dependent microbial sulfur oxidation strategies across diverse environments[J]. Frontiers in Microbiology, 2024;15.

[10] Mebane C A, Ivey C D, Wang N, et al. Direct and Delayed Mortality of Ceriodaphnia dubia and Rainbow Trout Following Time-Varying Acute Exposures to Zinc[J]. Environmental toxicology and chemistry, 2021;40(9):2484–98.

[11] Hirabayashi K, Sasaki E, Ohno H, et al. Enzymes that generate and regulate intracellular persulfides and polysulfides: mechanistic insights and inhibitors[J]. Frontiers in Physiology, 2026;Volume 17 - 2026.

[12] Maiti B K, Maia L B, Moura J J G. Sulfide and transition metals - A partnership for life[J]. Journal of inorganic biochemistry, 2022;227.

[13] Cirino G, Szabo C, Papapetropoulos A. Physiological roles of hydrogen sulfide in manmalian cells, tissues, and organs[J]. Physiological reviews, 2023;103(1):31–276.

[14] Guo J F, Shi C K, Yu C Y, et al. Protein S-sulfhydration: Mechanisms and therapeutic implications in Alzheimer's disease and Parkinson's disease[J]. Free radical biology and medicine, 2026;246:431–41.

[15] Morris J L, Lee J J, Morris R E, et al. Black gas, bright future: H_2S based therapeutics for neurodegenerative disorders[J]. Neurotherapeutics, 2025;22(6).

[16] Tripathi S J, Chakraborty S, Miller E, et al. Hydrogen sulfide signalling in neurodegenerative diseases[J]. British journal of pharmacology, 2026;183(1):83–100.

[17] Zhao X, Zhang J, Qiao J, et al. AIE on a chip: Quantifying polymer solution transport in porous media[J]. Sensors and Actuators B: Chemical, 2025;443:138246.

[18] Mita Y, Iwama T, Yu H, et al. Apparent Viscosity Measurement of Gas–liquid Multiphase Fluids by the Falling Ball Method[J]. ISIJ International, 2024;advpub.

[19] Wolak A, Zając G, Słowik T. Measuring Kinematic Viscosity of Engine Oils: A Comparison of Data Obtained from Four Different Devices[J]. Sensors, 2021. p. 2530.

[20] Minei P, Iasilli G, Ruggeri G, et al. Molecular Rotors with Aggregation-Induced Emission (AIE) as Fluorescent Probes for the Control of Polyurethane Synthesis[J]. Chemosensors, 2021;9(1).

[21] Wang H, Li X, Li J, et al. Synthesis of a “Turn-On” Mg^{2+} fluorescent probe and its application in hydrogel adsorption[J]. Journal of Molecular Structure. 2023;1281:135085.
[22] Aran G C, Bayraç A T. Fluorescence-based viscosity determination of corn starch using Auramine O[J]. Food chemistry, 2025;496.
[23] Ludescher R D, Komaiko J S, Corradini M G. Monoazo dyes as probes for bulk and local viscosity Potential applications in semi-solid foods[J]. Agro food industry Hi-teach, 2012;23(3):11–3.
[24] Ye C, Xiao N, Fan C L, et al. A NIR fluorescent probe for dual-phase viscosity monitoring in beverage thickeners and in vivo[J]. Spectrochimica acta part a-molecular and biomolecular spectroscopy, 2026;348.
[25] Zheng X Y, Zhong Z M, Feng C M, et al. Food quality surveillance: A smart fluorescent probe for viscosity-based spoilage detection[J]. Food chemistry, 2026;499.
[26] Dai Y P, Huang H, Gao H T, et al. Rational design of a 1,8-naphthalimide-based fluorescent probe and its application in liquid food detection of viscosity and living cells[J]. Journal of molecular structure, 2025;1340.
[27] Zheng M Y, Li Y M, Li M, et al. A long wavelength fluorescent probe for detecting viscosity and its application in liquid foods and bioimaging[J]. Food chemistry, 2025;482.
[28] Ceramella J, Iacopetta D, Catalano A, et al. A Review on the Antimicrobial Activity of Schiff Bases: Data Collection and Recent Studies[J]. Antibiotics-basel, 2022;11(2).
[29] Jorge J, Santos K F D, Timoteo F, et al. Recent Advances on the Antimicrobial Activities of Schiff Bases and their Metal Complexes: An Updated Overview[J]. Current medicinal chemistry, 2024;31(17):2330–44.
[30] Mukhtar S S, Hassan A S, Morsy N M, et al. Overview on Synthesis, Reactions, Applications, and Biological Activities of Schiff Bases[J]. Egyptian journal of chemistry, 2021;64(11):6541–54.

Supplementary Files

This is a list of supplementary files associated with this preprint. Click to download.

- SupportingInformation.docx